Taking it to the next level: Searching for gravitational waves with eccentricity from compact binary coalescences

Author: Elwin K. Y. Li[1],
Mentor: Alan J. Weinstein[2]
Hong Kong University of Science and Technology, Clear Water Bay, Kowloon, Hong Kong[1]
LIGO Laboratory, California Institute of Technology, Pasadena, CA 91125, USA[2]
Email: kyeliaa@connect.ust.hk[1], ajw@caltech.edu[2]
(Dated: July 14, 2023)

Gravitational waves (GWs)[1, 2] are fundamental predictions of general relativity. GW detections have introduced a novel window into the universe and are revolutionizing our understanding of astrophysics. The motion of two massive objects in an eccentric orbit emits GWs which carry information about the eccentricity of the binary black hole (BBH) source. These waveforms are characterized by their eccentricity, which measures the deviation of the orbit from a quasi-circular orbit. Studying eccentric binary orbits provides evidence for the dynamic formation of the binary system. In this project, we study a new family of GW waveforms from eccentric binaries and their implications for detecting and analyzing eccentric compact binary systems near mergers. I will develop eccentric waveform models and parameter estimation frameworks for eccentric BBH and use these tools to analyze the data from current and upcoming GW observations. Since eccentric waveforms are predicted to have similar waveforms with GWs from BBH systems with precessing, I will try to distinguish eccentric waveforms and precessing waveforms by investigating their differences. We will determine the minimum eccentricity that could be detectable with GWs as a function of SNR and other parameters.

I. INTRODUCTION AND MOTIVATION

A. Background

The discovery of GW, initially proposed by Einstein's theory of general relativity[3–6], has brought a new observational window on the cosmos. Exploring the properties of GW can provide us with fresh perspectives into the properties of massive compact objects (neutron stars and black holes) in the universe and their role in the evolution of galaxies.

B. Gravitational Waves

GWs are ripples in space-time, which propagate outward at the speed of light, generated by the acceleration of massive objects. BBH mergers and binary neutron star (BNS) mergers are compact binary coalescences (CBCs) that generate detectable gravitational waves. Since the distance of CBCs from Earth are extremely far, GWs generated are extremely weak and hard to detect by the time they reach the Earth. They were first predicted in 1916 from Einstein's General Theory of Relativity (GR). GWs have a property called polarization, which describes the orientation of the ripples. Just as electromagnetic waves have different polarizations (linear, circular, or elliptical), GW can also have different polarizations. GW has two transverse polarization modes: plus-polarization (h_+) and cross-polarization (h_+). The terms plus and the cross will be collectively known as the linear polarization basis. They stretch and compress the space-time in the two directions orthogonal to the direction of propagation[7]. h_+ is like the stretching and squeezing of space-time in GW with a 45-degree angle. The impact on test particles in a h_x GW would be similar to that of a regular polarized GW but with a 45-degree rotation.

C. Gravitational Wave Detectors

Nowadays, gravitational waves can be detected by gravitational waves observatories[8], including Advanced LIGO (aLIGO)[9], VIRGO[10], and Kagra[11], which already have conducted three observing runs[12–14] in total. Figure 1 shows the configuration of the laser interferometer at the heart of the LIGO detectors and the laser mirrors (test masses) on their quadruple-pendulum suspensions. Since the two arms have the same nominal length, the split laser beams will have destructive interference at the output port when joined at the beam splitter, and the detector will register no signal. When GW passes through the detector, the arms will be stretched or compressed, resulting in length differences. The interference pattern will then be partially constructive such that a weak signal can be detected at the output port.

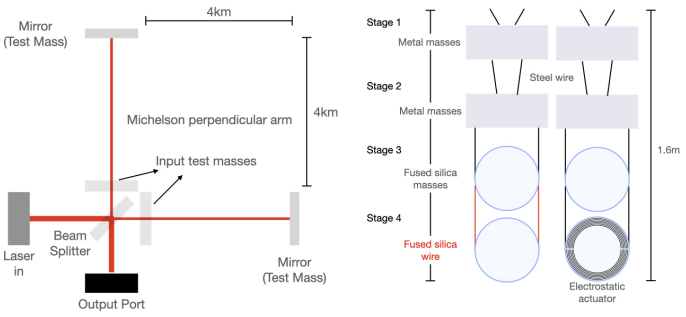

Figure 1. Interferometer configuration (Left) and test mass setup (Right).

D. Eccentric Binaries

When two massive objects move in an eccentric orbit, they generate GW waveforms that encode the eccentricity - eccentric waveforms. The eccentricity of these waveforms reflects the extent of orbit deviation from a perfect circle. For a quasi-circular orbit (since eccentricity = 0), there are fifteen parameters (sixteen for BNS) to determine a GW, including the masses of the two mergers, the spin of the two mergers in three different directions (x, y, and z directions for both compact objects), source distance, sky location (right ascension and declination), coalescence time, coalescence phase, inclination and polarization (and tidal deformability for BNS), in which eccentricity is not one of the parameters. Since GWs are dominantly quadrupolar radiation, the frequencies of GW (f_{GW}) are doubled that of the orbital frequencies (f_{orb}). Our detectors cannot detect GW when f_{GW} is lower than 20Hz. The problem is that the orbit could be eccentric initially but become less eccentric or nearly circular when the two sources are getting close with an orbital frequency higher than 20Hz. If the eccentricity is high at $f_{GW} = 20$Hz, it is predicted to approach zero by the time $f_{orb} = 50$Hz.

BBHs are common in the universe. BBH systems may form through common evolution in isolation (first column of Fig 2). Another possibility is dynamical capture, in which the binary system is formed by capturing other massive objects (second column in Fig. 2). Other formation mechanisms are predicted as well. We do not know which of these formation mechanisms are dominant for systems that merge in the LIGO frequency band.

In GW astrophysics, it is important to investigate eccentric gravitational waveforms as they can offer valuable information about the formation characteristics of BBH. Several studies[15, 16] have been conducted on eccentric gravitational waveforms based on the standard approach and a novel method suggested[17], which uses parameter estimation. These investigations offer new perspectives into the characteristics of these waveforms and their possible uses in examining the cosmos.

E. BBH Formation in Isolation and Dynamic Capture

One of our primary goals is to understand how compact binary systems form. One possibility is the BBH Formation in Isolation, in which a binary system evolves together from the start, undergoes Roche lobe overflow and a common envelope stage that tightens the binary orbit through dynamical friction. One of the stars will directly turn into a black hole. If a common envelope occurs, the giant envelope will surround the orbit of the system. Thermal energy is transferred to the envelope and may trigger the ejection of the envelope. Once the ejection of the envelope occurs, the massive star will directly turn into a black hole, leading to the inspiral of the two black holes and merging into a single one at the end. This BBH formation and merger is a common evolution in which the orbit is quasi-circular, with eccentricity close to zero. Another possibility is BBH formation in dense star clusters (e.g., at the center of galaxies or in globular clusters) through dynamic capture. The binary massive star system undergoes a similar process as the BBH formation in isolation unless another massive BH is captured by the cross-section area of the two stars, ejecting the massive stars out of the original orbit and forming a new BBH system.[18] Since the new-coming BH removed some orbital energy from the original orbit, the period can be decreased from ten trillion to less than ten minutes, leading to a highly eccentric orbit. Figure 2 shows the evolution of the two BBH formation mechanisms. The probability of dynamic capture depends on the capture cross-section. The study of eccentric GWs provides valuable information to determine which form of BBH system dominates. We also want to look for dynamic capture with a very small cross-section such that the time of the merger is within seconds.

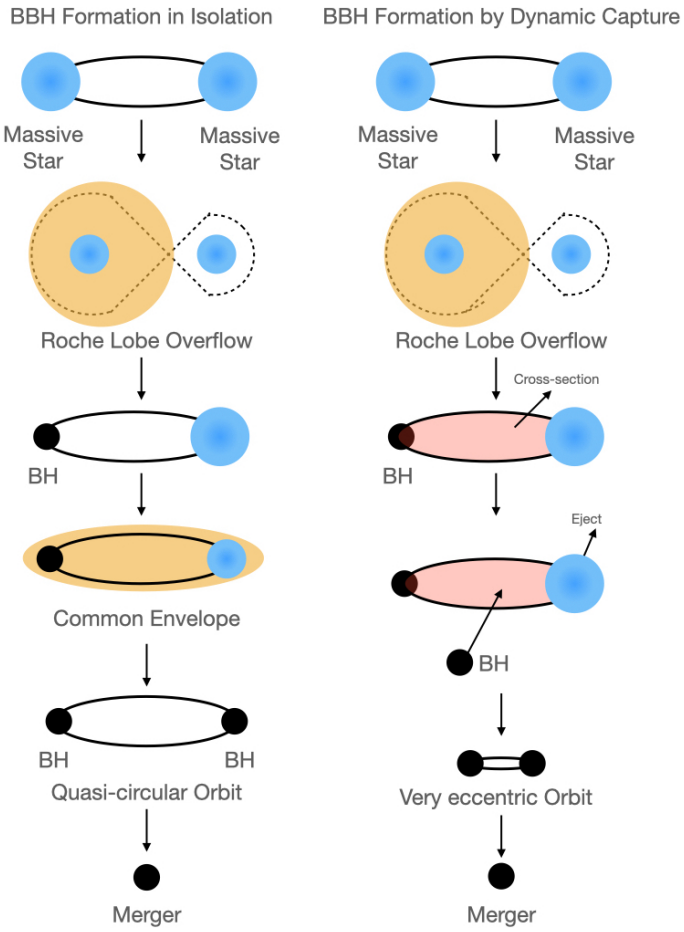

Figure 2. Following Michela Mapelli et al., BBH Formation in Isolation (Left) and by Dynamic Capture (Right).

F. Matched-filtering

Matched-filtering[19], with PyCBC[20–22] search pipeline is a technique that can detect numerous possible GW candidates from a given period with similar shapes. It can detect signals from stationary Gaussian noise. Suppose $n(t)$ is

the stationary Gaussian noise process, $S_n(f)$ is the one-sided power spectral density (PSD), the matched-filtering output of a data stream is

$$x(t_0) = 2\int_{-\infty}^{\infty} \frac{\tilde{s}(f)\tilde{h}^*_{template}(f)}{S_n(f)}df \tag{1}$$

which may only contain noise $s(t) = n(t)$, or signal with noise $s(t) = n(t) + h(t)$ where $h(t)$ is the signal. Denote $h_{template}(t)$ as the filter template. Since there are unknown parameters (amplitude, coalescence phase, and binary com[anion masses) in the waveform, the "best match" unknown phase ϕ_0 has to be found by maximizing $x(t_0)$ over ϕ_0.

$$x(t_0) = x_{re}(t_0)cos2\phi_0 + x_{im}(t_0)sin2\phi_0, \tag{2}$$

where $x_{re,im}$ can be found by using Eq. 1 or Eq. 2 with $\phi_0 = 0$. Therefore, the maximum can be found in

$$x^2(t_0)|_{\hat{\phi_0}maximum} = x^2_{re}(t_0) + x^2_{i,}(t_0) \tag{3}$$

at $2\hat{\phi_0} = arg(x_{re} + ix_{im})$. The modulus of complex filter output then gives the maximum:

$$z(t_0) = x_{re}(t_0) + ix_{im}(t_0) \tag{4}$$

$$= 4\mathbb{R}\int_0^{\infty} \frac{\tilde{s}(f)(\tilde{h}^*_{template}(f))_0}{S_n(f)}e^{2\pi i f t_0}df, \tag{5}$$

where $(\tilde{h}^*_{template}(f))_0 = (\tilde{h}^*_{template}(f))_{t_0=0,\phi_0=0}$. The normalization constant for each template is calculated by

$$\sigma^2_m = 4\int_0^{\infty} \frac{|\tilde{h}_{1Mpc,m}(f)|^2}{S_n(f)}df, \tag{6}$$

such that the signal-to-noise ratio can be calculated afterward. the Amplitude signal-to-noise ratio of the quadrature matched-filtering is given by

$$\rho_m(t) = \frac{|z_m(t)|}{\sigma_m}. \tag{7}$$

If the signal is absent, then

$$< \rho^2_m >= 2. \tag{8}$$

Since for purely static and Gaussian noise, it is improbable to obtain $\rho_m >> 1$, a lower threshold on ρ_m is often used to identify event candidates.

Finally, for each trigger, a False-Alarm-Probability (FAP), which is the probability that noise can produce a trigger with a ranking statistic $\ln \mathcal{L} \geq \ln \mathcal{L}^*$, will be calculated as

$$\mathbf{FAP} = P(\ln \mathcal{L} > \ln \mathcal{L}^*|\mathbf{noise}) = \int_{\ln \mathcal{L}^*}^{\infty} P(\ln \mathcal{L}|\mathbf{noise})d\ln \mathcal{L} \tag{9}$$

The lower the FAP, the more likely the trigger comes from an actual GW signal.

II. OBJECTIVE

The proposed research aims to evaluate the properties of existing and newly-developed GW waveforms that incorporate the effects of non-zero eccentricity in the binary orbit. The effect of eccentricity on GW waveforms and their detectability in LIGO has been shown in past studies[23],[24]. The existing data will be analyzed to compare eccentric and non-eccentric waveforms, and more detailed studies regarding this parameter will be conducted. This research will also analyze existing data and compare eccentric and non-eccentric waveforms to achieve these goals. This will provide insights into the effects of eccentricity on the waveform, which will then be used to conduct more in-depth studies on this parameter.

According to the study conducted by Philip Carl Peters[25], the time average of the rate of change of eccentricity of the orbit is given by:

$$\langle \frac{de}{dt} \rangle = -\frac{304eG^3m_1m_2(m_1+m_2)}{15c^5a^4(1-e^2)^{5/2}}(1 + \frac{121e^2}{304}). \tag{10}$$

Using this equation, we can evolve the eccentricity of eccentric BBH orbit as it inspirals and approaches merger.

In the coming research period, I will study eccentric waveforms in the following aspects:

1. Do the eccentric waveforms pass a set of Sanity checks in which they look reasonable and have proper limiting behavior?
2. Comparison between eccentric and non-eccentric waveforms.
3. Is it possible to find the eccentric waveform using a quasi-circular waveform in our template bank?
4. Find out the minimum eccentricity with which the eccentric waveform cannot be distinguished from a regular waveform.
5. By investigating their differences, try to distinguish eccentric waveforms and precessing waveforms.
6. How does the eccentricity evolve with time as the binary system approaches merger?
7. What do eccentric waveforms look like in the time and frequency domain?
8. Develop a framework to calculate the eccentricity value when constructing parameter estimation.
9. How can eccentric waveforms be searched with parameter estimation?

Since current research regarding eccentric gravitational waveforms only considers small eccentricity, studying eccentricity in gravitational waveforms, regardless of its magnitude, is crucial as it can provide a more comprehensive understanding of the behavior of compact binary systems in a broader range of eccentricities. This research can shed light on the

physics behind the inspiral and merger of binaries with higher eccentricities, which can lead to the detection of more GW signals from such systems. Moreover, it can help improve our existing models for the dynamics of compact binaries, which can lead to more accurate parameter estimation and GW detection. Studying high eccentricities can also help us understand the astrophysical processes responsible for producing such systems and their implications for cosmology and astrophysics. Therefore, this research can have significant implications for understanding the universe and the properties of compact objects such as neutron stars and black holes.

III. METHODS

To conduct this study, simulated eccentric waveforms with different magnitudes of eccentricity will be generated. These waveforms will be compared to standard quasi-circular waveforms using matched-filtering and sanity checks to identify apparent differences. The study of eccentric waveforms involves using waveform overlap with standard waveforms. By comparing them, we can quantify the waveforms using parameter estimation, ensuring that eccentricity is considered when generating or detecting GW signals. Any waveforms with apparent differences from regular waveforms will be saved for further usage, including the construction of an eccentric waveform template bank.

The next step involves performing an injection study to determine the minimum eccentricity with which the eccentric waveform can be distinguished from a regular waveform. This involves injecting a simulated eccentric waveform into a random signal and attempting to use a non-eccentric waveform template to recover it.

The injection study will allow researchers to understand better the properties of eccentric waveforms and how they differ from regular waveforms. This information can then be used to improve the detection of GW from eccentric sources, such as binary systems with large eccentricities.

I will study eccentric waveforms by the following steps in short:

1. Generate eccentric and non-eccentric waveforms
2. Compare the waveforms
3. Quantify the waveform overlaps
4. Compute and plot the match in both the time and frequency domain
5. Repeat Steps 1 to 4 for similar eccentricity
6. Repeat Steps 1 to 4 for precessing waveforms
7. Construct a 1D simulation which search for the signal with random eccentricity which is injected to random Gaussian noise
8. Calculate the likelihood between the injected signal and the best-matched template waveform
9. Construct a 2D and 3D simulation similar to Step 7 with two and three unknowns respectively
10. Construct a search pipeline which can be used for searching eccentric waveforms in real data

IV. TIMELINE

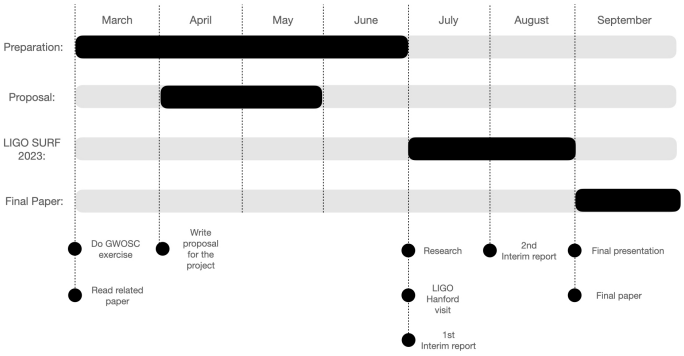

Figure 3. Timeline of this proposed project.

In the past four weeks, the newly-developed waveforms, TEOBResumS, have been studied and reviewed to check their precision and accuracy in simulating an eccentric GW waveform. A simple simulation is being constructed to compare eccentric waveforms with non-eccentric waveforms and precessing waveforms and calculate the matches between them. Another simulation is under construction to inject an eccentric waveform into a random Gaussian noise and search for the waveforms and their eccentricity value by matched filtering to study detectability. A preliminary model for searching for eccentric waveforms from real data is also being constructed without testing. In the coming six weeks, the accuracy of the TEOBResumS waveform model will be finalized by comparing it with the Simulating eXtreme Spacetimes (SXS) templates[26, 27]. Bilby[28] will be used to calculate the matched-filtering and calculate the signal-to-noise ratio (SNR) and the likelihood of the injected eccentric waveforms. It will also be used to do 2D and 3D matches in which the masses of the binaries and the mass ratios are kept unknown before injecting the waveform into random noise. The simulation will be further modified and used to search for eccentric GWs in real data after a series of comprehensive tests.

V. PROGRESS UPDATE

Eccentric waveforms are the key to my research. Generally, there are three different templates of waveforms, the post-Newtonian template[29], the SXS templates, and the TEOBResumS templates[30, 31]. Only templates from SXS and TEOBResumS can be eccentric. TEOBResumS templates are new and are currently not used for data analysis in LIGO. However, eccentric waveforms from SXS are limited. To generate waveforms with different eccentricities for my search,

it is necessary to review the precision of the TEOBResumS templates.

A. Reviewing the TEOBResumS Waveforms

To review the precision of the TEOBResumS waveforms, I first generate waveforms with different eccentricities and mass ratios to perform sanity checks. Throughout the checking, it is found that waveforms with eccentricity equal to or larger than 0.9999 will blow up. Only a straight line instead of a waveform will be plotted (Figure 4).

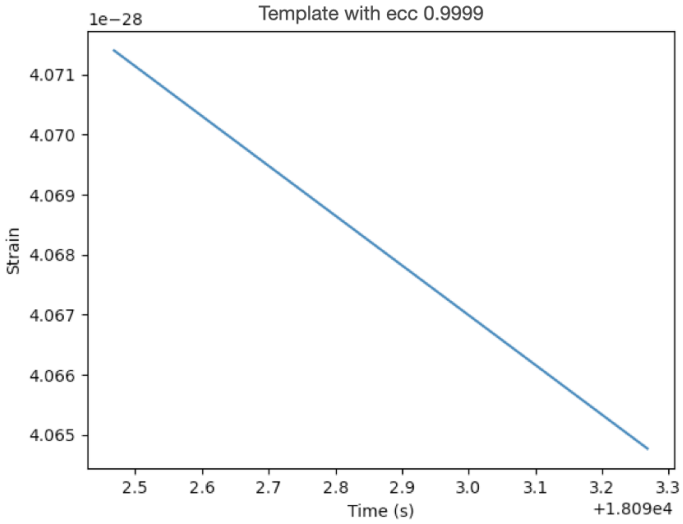

Figure 4. Blown up waveform of eccentricity 0.9999.

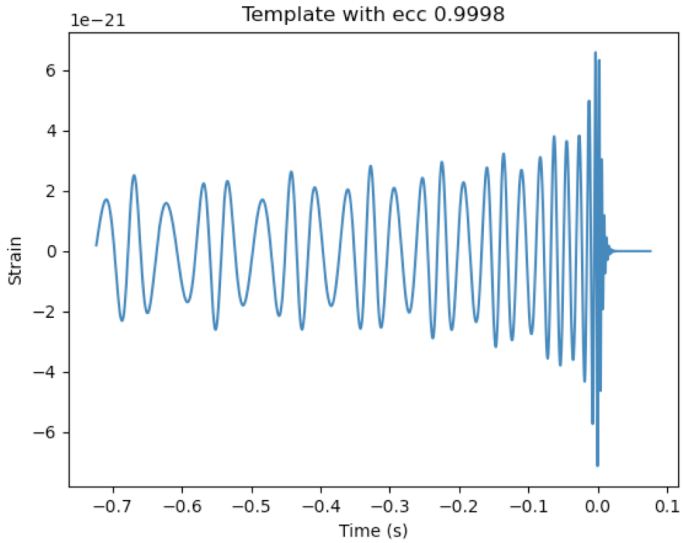

Figure 5. Complete waveform of eccentricity 0.9998.

The mass ratio limit is also tested by increasing the mass ratio until the plot of the waveform in the time domain becomes unusual. It is shown that for low-pass GW frequency 15.0Hz, a waveform with a mass ratio of 4.0 can barely be shown with a duration of around 0.8 seconds from inspiral to ringdown. If the low-pass GW frequency is set to be 1.0Hz, a waveform with a mass ratio of 150.0 can also be plotted. This shows that the TEOBResumS waveform is useable even with a very high mass ratio. Since the minimum detectable frequency in the LIGO frequency band is about 20Hz, the TEOBResumS template shows compatibility with LIGO currently.

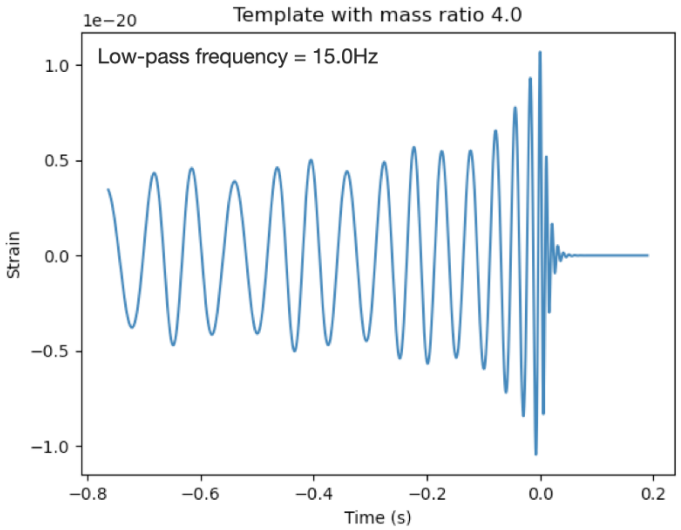

Figure 6. Waveform with mass ration 4.0 and low-pass frequency 15.0Hz.

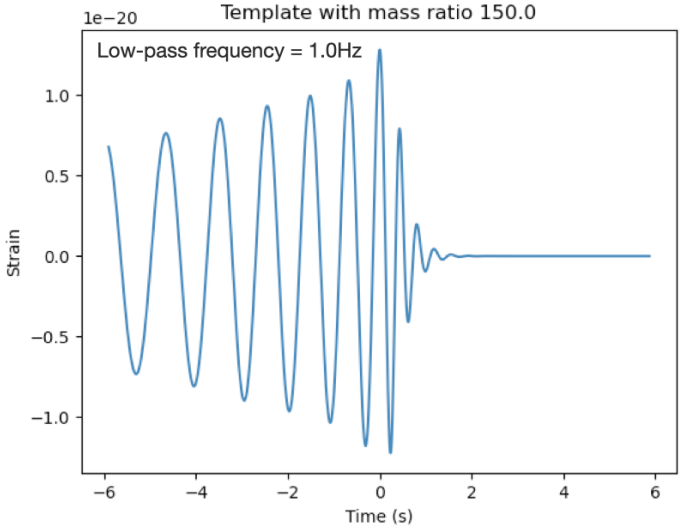

Figure 7. Waveform with mass ration 150.0 and low-pass frequency 1.0Hz.

B. Waveform Overlap Matching Model

A simple matching model is being constructed to do waveform overlapping and match calculating between pairs of eccentric waveforms and non-eccentric waveforms and pairs of

eccentric waveforms and precessing waveforms in both the time domain and frequency domain. The simulation uses waveforms with different eccentricities to do the overlapping and calculate the match. After calculating the matches, graphs of the match against the eccentricity of the testing waveform are plotted.

1. *Eccentric Waveforms and Non-eccentric Waveforms Comparison*

From the plots, it is shown that the comparing processes in the time domain and frequency domain give similar results in calculating the matches. The larger the eccentricity of the eccentric waveform, the smaller the match value with the non-eccentric waveform. It is also shown that the result of the matching is the most significant in extreme eccentricity values (eccentricity nearest to 0.0 or 1.0). The match values fluctuate a lot if the eccentricity of the waveform being overlapped is not extreme. This implies that the accuracy of searching eccentric waveforms with non-extreme eccentricities will be challenging with the existence of noise.

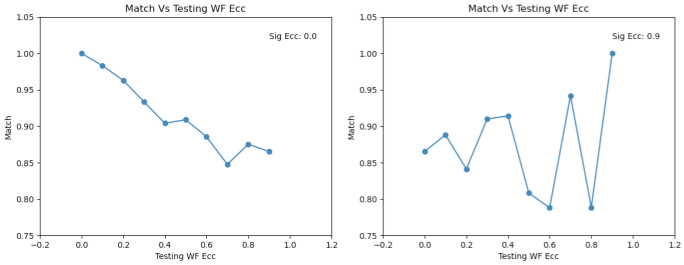

Figure 8. Match values against Eccentricity of testing waveforms in time domain (Left: Eccentricity of signal = 0.0. Right: Eccentricity of signal = 0.9).

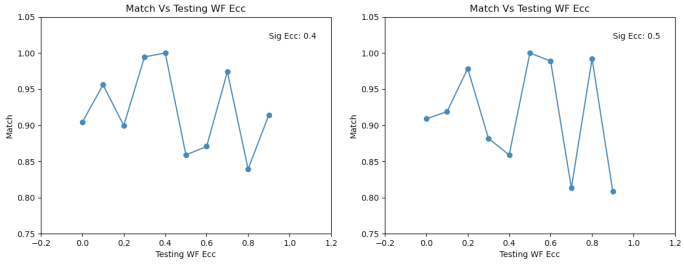

Figure 9. Match values against Eccentricity of testing waveforms in time domain (Left: Eccentricity of signal = 0.4. Right: Eccentricity of signal = 0.5).

2. *Eccentric Waveforms and Precessing Waveforms*

Match values are being calculated between waveforms with different eccentricity and waveforms with different magnitudes of spins of the binaries. From the plots, it is possible for

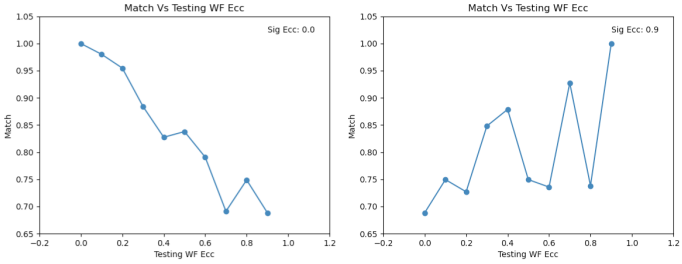

Figure 10. Match values against Eccentricity of testing waveforms in frequency domain (Left: Eccentricity of signal = 0.0. Right: Eccentricity of signal = 0.9).

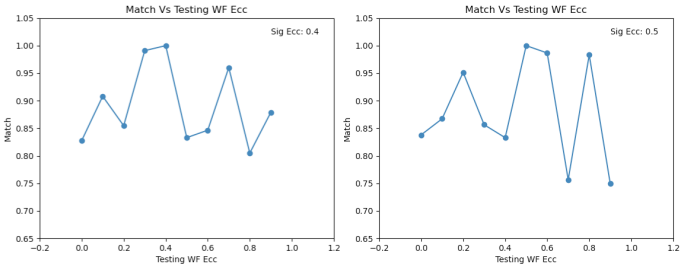

Figure 11. Match values against Eccentricity of testing waveforms in frequency domain (Left: Eccentricity of signal = 0.4. Right: Eccentricity of signal = 0.5).

waveforms with eccentricity to have a matching value with precessing waveforms. Currently, it is impossible to ensure whether the differences between eccentric waveforms and precessing waveforms can be spotted, and the issue will be further investigated by testing a more comprehensive range of precessing waveforms.

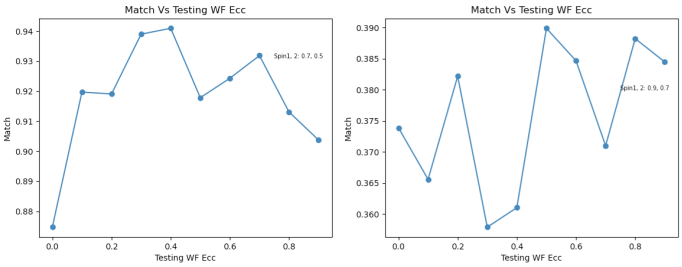

Figure 12. Match values against Eccentricity of testing waveforms in time domain (Left: Waveform with eccentricity 0.4 is highly matched with the precessing waveform. Right: The precessing waveform is independent to the eccentric waveform).

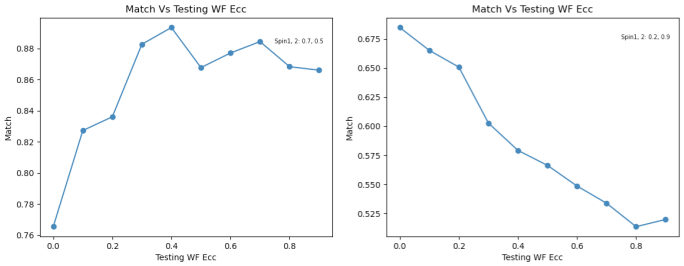

Figure 13. Match values against Eccentricity of testing waveforms in frequency domain (Left: Waveform with eccentricity 0.4 is highly matched with the precessing waveform. Right: The precessing waveform is independent to the eccentric waveform).

VI. REFERENCES

[1] I. Chakrabarty, (1999), arXiv:physics/9908041 [physics.ed-ph].
[2] M. Spurio, (2019), arXiv:1906.03643 [astro-ph.HE].
[3] J. W. van Holten, Universe **9**, 110 (2023), arXiv:2211.10123 [gr-qc].
[4] M. Le Delliou (2022) arXiv:2208.02506 [gr-qc].
[5] J. F. Pommaret, arXiv e-prints , arXiv:2302.06585 (2023), arXiv:2302.06585 [math.GM].
[6] G. Nash, (2023), 10.1142/S0218271823500311, arXiv:2304.09671 [gr-qc].
[7] M. Isi, (2022), arXiv:2208.03372 [gr-qc].
[8] R. Abbott *et al.* (KAGRA, VIRGO, LIGO Scientific), Phys. Rev. X **13**, 011048 (2023), arXiv:2111.03634 [astro-ph.HE].
[9] J. Aasi *et al.* (LIGO Scientific), Class. Quant. Grav. **32**, 074001 (2015), arXiv:1411.4547 [gr-qc].
[10] F. Acernese *et al.* (VIRGO), Class. Quant. Grav. **32**, 024001 (2015), arXiv:1408.3978 [gr-qc].
[11] K. Somiya (KAGRA), Class. Quant. Grav. **29**, 124007 (2012), arXiv:1111.7185 [gr-qc].
[12] B. P. Abbott *et al.* (LIGO Scientific, Virgo), Phys. Rev. X **9**, 031040 (2019), arXiv:1811.12907 [astro-ph.HE].
[13] R. Abbott *et al.* (LIGO Scientific, Virgo), Phys. Rev. X **11**, 021053 (2021), arXiv:2010.14527 [gr-qc].
[14] R. Abbott *et al.* (LIGO Scientific, VIRGO, KAGRA), (2021), arXiv:2111.03606 [gr-qc].
[15] B. P. Abbott *et al.* (LIGO Scientific, Virgo), Astrophys. J. **883**, 149 (2019), arXiv:1907.09384 [astro-ph.HE].
[16] T. Yang, R.-G. Cai, Z. Cao, and H. M. Lee, Phys. Rev. D **107**, 043539 (2023), arXiv:2212.11131 [gr-qc].
[17] S. Schmidt, B. Gadre, and S. Caudill, (2023), arXiv:2302.00436 [gr-qc].
[18] M. Mapelli, Front. Astron. Space Sci. **7** (2020).
[19] B. Allen, W. G. Anderson, P. R. Brady, D. A. Brown, and J. D. E. Creighton, Phys. Rev. D **85**, 122006 (2012), arXiv:gr-qc/0509116.
[20] K. Chandra, V. Villa-Ortega, T. Dent, C. McIsaac, A. Pai, I. W. Harry, G. S. C. Davies, and K. Soni, Phys. Rev. D **104**, 042004 (2021), arXiv:2106.00193 [gr-qc].
[21] S. A. Usman *et al.*, Class. Quant. Grav. **33**, 215004 (2016), arXiv:1508.02357 [gr-qc].
[22] D. Davis, M. Trevor, S. Mozzon, and L. K. Nuttall, Phys. Rev. D **106**, 102006 (2022), arXiv:2204.03091 [gr-qc].
[23] E. A. Huerta, P. Kumar, S. T. McWilliams, R. O'Shaughnessy, and N. Yunes, Phys. Rev. D **90**, 084016 (2014), arXiv:1408.3406 [gr-qc].
[24] S. Tanay, M. Haney, and A. Gopakumar, Phys. Rev. D **93**, 064031 (2016), arXiv:1602.03081 [gr-qc].
[25] P. C. Peters, Phys. Rev. **136**, B1224 (1964).
[26] M. Boyle *et al.*, Class. Quant. Grav. **36**, 195006 (2019), arXiv:1904.04831 [gr-qc].
[27] A. H. Mroue *et al.*, Phys. Rev. Lett. **111**, 241104 (2013), arXiv:1304.6077 [gr-qc].
[28] G. Ashton *et al.*, Astrophys. J. Suppl. **241**, 27 (2019), arXiv:1811.02042 [astro-ph.IM].
[29] S. Isoyama, R. Sturani, and H. Nakano, (2020), 10.1007/978-981-15-4702-7$_3$1 − 1, arXiv:2012.01350 [gr-qc].
[30] D. Chiaramello and A. Nagar, Phys. Rev. D **101**, 101501 (2020), arXiv:2001.11736 [gr-qc].
[31] A. V. Joshi, S. G. Rosofsky, R. Haas, and E. A. Huerta, Phys. Rev. D **107**, 064038 (2023), arXiv:2210.01852 [gr-qc].